Asian Journal of Chemistry; Vol. 38, No. 4 (2026), 1002-1006

ASIAN JOURNAL OF CHEMISTRY

https://doi.org/10.14233/ajchem.2026.35573

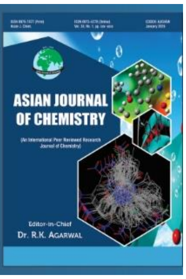

Structural, Photoluminescence and Colorific Properties of Sm^{3+} doped $ZnMoO_4$ Phosphors for Warm White LEDs

M. MALLIKARJUNA[1], THUMMALA CHENGAIAH[1,*], Y. BABY[1],
G. MOULIKA[2] and BORELLI DEVA PRASAD RAJU[1,*]

[1]Department of Physics, Sri Venkareswara University, Tirupati-517502, India
[2]Department of Physics, Dravidian University College of Engineering, Kuppam-517426, India

*Corresponding authors: E-mail: chengaiahphysics@gmail.com; drdevaprasadraju@gmail.com

Received: 7 January 2026 *Accepted*: 18 February 2026 *Published online*: 8 April 2026 AJC-22321

Zinc molybdates ($ZnMoO_4$) phosphors activated with different samarium (Sm^{3+}) amounts (0.5, 1.0, 1.5 and 2.0 mol%) were synthesised using a low temperature initiated citrate gel combustion process. The crystal structure of $ZnMoO_4$:Sm^{3+} phosphors were analysed by XRD and their size was determined to be approximately 20 nm by the Scherrer equation. The FTIR spectral studies confirmed the presence of the distinct functional groups in the prepared phosphors. When the n-UV was excited to 402 nm, four emission maxima (PL) were detected at 567, 602, 649 and 708 nm. These were linked to the Sm^{3+} ion transitions: $^4G_{5/2}\rightarrow{}^6H_{5/2}$ (yellow), $^6H_{7/2}$ (orange), $^6H_{9/2}$ (reddish orange) and $^6H_{11/2}$ (red). Dexter and Shulman's theory studied the multipolar interaction that causes photoluminescence (PL) quenching *via* dipole-dipole type interaction in the present $ZnMoO_4$:Sm^{3+} phosphors. The double-exponential function was used to fit the decay curves of the prepared phosphors and their lifetimes were found to be 1.23, 1.19, 1.11 and 1.09 ms. The colorimetric characteristics, which span the values (x, y) of 0.60 and 0.40, the colour purity of 96% and the colour temperatures below 2000 K, indicate that the fluorescent materials $ZnMoO_4$:Sm^{3+} have great potential for use in light-emitting diodes (warm-LEDs).

Keywords: Samarium, $ZnMoO_4$ phosphors, Crystal structure-XRD, Photoluminescence, Decay curves, Colorific properties.

INTRODUCTION

The upgrade of optical communications and the development of integrated electronics require a new category of luminescent materials, which have been effectively used for light emitting devices (LEDs) [1-4]. As a result, the era of modern lighting technology can be composed of a white-LED with blue LED and yellow emitting phosphor. However, the technique of producing white light through various LEDs elevates production costs and low colour rendition due to the absence of red-emitting elements. In this regard, researchers have synthesised several phosphor materials activated with Sm^{3+} ions as a solution to existing red-emission limitations. In view of that, $Ba_2La_2ZnW_2O_{12}$:Sm^{3+} [5], $ZnAl_2O_4$:Sm^{3+} [6], $LiCaBO_3$:Sm^{3+} [3], KYBO:Sm^{3+} [7] and $LiCa_3ZnV_3O_{12}$:Sm^{3+} [4] have been widely investigated for reddish-orange emitting LED applications. Similarly, new phosphors activated with Sm^{3+} ions still need to be explored to overcome the deficiency of red components through excitation of UV/blue wavelengths.

Among the different oxide based inorganic phosphors, molybdates (MoO_4) have been ideal properties such as high solubility of RE^{3+}, near ultraviolet absorption, wideband blue emission, high thermal and chemical stability [8,9]. Four O^{2-} ions with approximately tetrahedral symmetry surround the core Mo metal ion, making $(MoO_4)^{2-}$ a very stable host element for rare-earth (RE^{3+}) activators [10,11]. Further, the absorbed energy of MoO_4^{2-} is transferred to the RE^{3+} activators, since the Mo–O bond has a broad and strong absorption band in the near ultraviolet (n-UV) range [9]. In this study, zinc molybdate ($ZnMoO_4$) by doping of Sm^{3+} activator was selected as a host material. When doped with Sm^{3+} ions, the wolframite-type of $ZnMoO_4$ with triclinic structure has high ability to improve the efficiency of lasers, optoelectronic devices, electrochemical and catalysis, scintillator [9,11-14]. Among different RE^{3+} ions, Sm^{3+} ion provides reddish-orange emission due to $^4G_{5/2}\rightarrow{}^6H_{11/2,9/2,7/2,5/2}$ (*J* = 11, 9, 7 and 5) transitions [15-18]. Also, the n-UV absorption (403 nm) of Sm^{3+} ions compatible with blue-emitting InGaN and GaN chips and thus the present

---

Sm^{3+} activated $ZnMoO_4$ phosphor can be used for the realisation of w-LED fabrication [8,19]. Due to the small ionic radius of Zn^{2+} (0.90 Å), the Zn^{2+} can easily occupy interstitial sites and affect the crystal field around the Sm^{3+} ion (1.079 Å) by rising the asymmetry [8]. Therefore, the incorporation of the Zn^{2+} transition metal into MoO_4 can improve the emission properties of the Sm^{3+} ion [8,20].

The goal of this study is to synthesize $ZnMoO_4$, which emits a reddish orange colour and contains various amounts of Sm^{3+} ions, using a simple, low-temperature method of citrate gel combustion process. A study on the structural and spectral characteristics of the current $ZnMoO_4$:Sm^{3+} phosphors was conducted using functional group analysis Fourier transform in infrared (FT-IR), X-ray diffraction (XRD) and excitation, emission and decay curves. Dexter & Schulman's theory was used to explain the multipolar interaction in relation to the photoluminescence (PL) breakdown of the phosphors $ZnMoO_4$:Sm^{3+}. An analysis of the implementation and characteristics of the white LEDs was conducted, considering their colour correction temperature (CCT), colour purity (CP) and colour coordinates (x, y).

EXPERIMENTAL

Phosphors $Zn(1–x)MoO_4$:xSm^{3+} were synthesised using a modified combustion process in citrate gel in various Sm^{3+} ion proportions (x = 0.5, 1.0, 1.5 and 2.0 mol%). The first materials used were highly pure (99.99%) chemical compounds such as ZnO (quality A.R.), $C_6H_8O_7$ (citric acid), Sm_2O_3 and $(NH_4)_6Mo_7O_{24}\cdot 4H_2O$, which were obtained from Sigma-Aldrich. In a conventional experiment, $ZnMoO_4$ was synthesised by dissolving standard amounts of each carbonate and oxide in 1 M conc. HNO_3. Nitrate precursors and electrical acid were mixed in a 1:2 molar ratio and the mixture was then dissolved in water. Citric acid serves as the monomer, facilitating the formation of a transparent complex gel after a drying period of 2 h in a furnace set at 75 °C. The gel was then placed in a quartz container and heated to 900 °C. Initially, the citrate complex produces a black, porous material that expands to nearly ten times the volume of the original gel, which subsequently decomposes, releasing H_2O and CO_2 vapours. A white huge mass of $ZnMoO_4$:Sm^{3+} nanophosphor was obtained after 15 min and could be easily crushed into an ultra-fine powder suitable for optical characterization. This method enables the efficient production of nanofiber particles with well-controlled sizes, with yields reaching around 90%.

Characterization: An X-ray Seifert diffractometer operating with Cu$K\alpha$ radiation (λ = 1.5406 Å) was used to analyze the crystal structure of $ZnMoO_4$:Sm^{3+}. This device operates in a range of 20º to 60º (2θ) at 40 kV and 30 mA. The FT-IR spectra were obtained using a Thermo Nicolet IR200 spectrophotometer. The photoluminescence excitation (PLE), photoluminescence (PL) and decline curves were obtained using a Jobin YVON Fluorolog-3 spectrofluorometer built on an arc lamp to xenon.

RESULTS AND DISCUSSION

XRD studies: The XRD patterns for $ZnMoO_4$ phosphors activated with 1.0 mol% Sm^{3+} and $ZnMoO_4$ phosphors are shown in Fig. 1. The diffraction peaks of samples location matches the appropriate positions shown in the JCPDS card No. 35-0765 and indicates the triclinic structure with space group $P\bar{1}$, no. 2. The mean crystallite size of prepared phosphors can be calculated using the Scherrer's equation [3,21]:

$$D_{hkl} = \frac{0.98\lambda}{\beta_{2\theta}\cos\theta} \qquad (1)$$

By substituting the XRD data of different peaks in eqn. 1, it was found that the average crystallite size of the $ZnMoO_4$:Sm^{3+} phosphors was approximately 20 nm. The discoveries show that all of the produced $ZnMoO_4$ phosphors are phase-dependent and that the activator ion Sm^{3+} had no discernible effect on the crystal structure of the synthesised phosphorus.

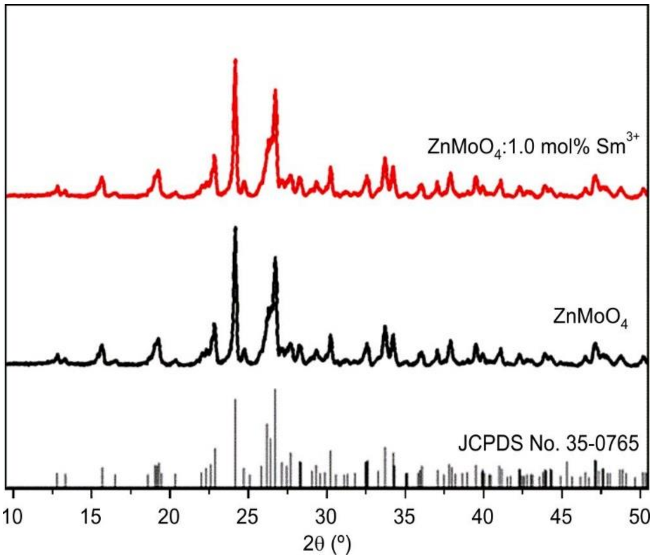

Fig. 1. XRD patterns of $ZnMoO_4$ phosphors activated with and without Sm^{3+} ions

FTIR spectral studies: Fig. 2 shows the FTIR spectra of $ZnMoO_4$ activated with various Sm^{3+} concentrations as well as those of $ZnMoO_4$ without dosage. The FTIR spectra of $ZnMoO_4$ phosphors show no significant shift in peak positions with increasing Sm^{3+} content. This suggests that the host lattice does not undergo any structural alterations in response to varying Sm^{3+} amounts. From Fig. 2, the Zn–O–Mo bending and stretching vibrational modes are mainly exhibited in the region 1000-700 cm^{-1} [22,23]. The band cantered at 864 cm^{-1} is assigned to the stretching and bending vibrations of Mo–O [23,24]. The O-H stretching and H–O–H bending vibrations are appeared at 3425 cm^{-1} and 1631 cm^{-1}, respectively [25].

PLE and PL spectral studies: As shown in Fig. 3, the PLE spectra of $ZnMoO_4$ activated with various Sm^{3+} doses (0.5, 1.0, 1.5 and 2.0 mol%) were analysed in the range of 350 to 570 nm, with an emission fixed at 602 nm. The $ZnMoO_4$:Sm^{3+} phosphors exhibited several PLE exhibits peaks in 344, 362, 375, 402, 418, 440, 475, 500, 528 and 561 nm due to the transition of levels from the $^6H_{5/2}$ to the subsequent levels. The

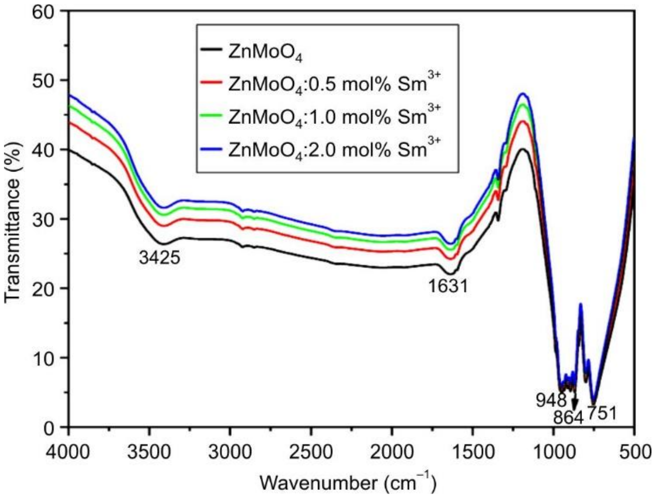

Fig. 2. FTIR spectra of ZnMoO$_4$ phosphors having varying amount of Sm^{3+}

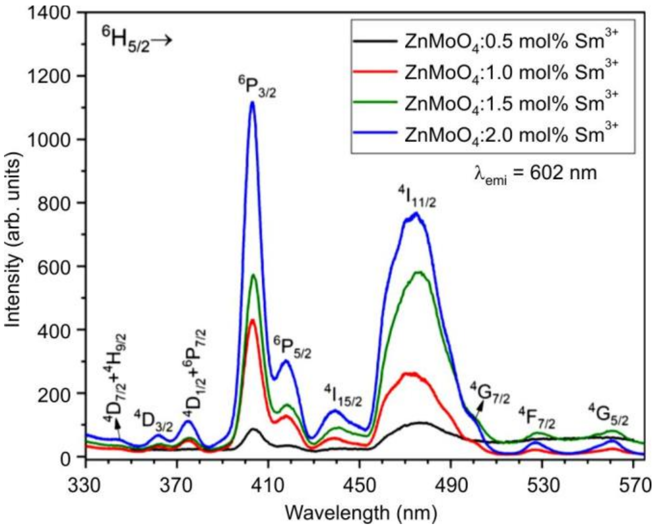

Fig. 3. PLE spectra of ZnMoO$_4$ phosphors activated with various Sm^{3+} amounts

levels are as follows: $^4D_{7/2}$+$^4H_{9/2}$; $^4D_{3/2}$; $^4D_{1/2}$+$^6P_{7/2}$; $^6P_{3/2}$; $^6P_{5/2}$; $^4G_{9/2}$; $^4I_{11/2}$; $^4G_{7/2}$; $^4F_{7/2}$; and $^4G_{5/2}$. In addition to the previously reported PLE peaks [26], a prominent excitation peak at 402 nm corresponding to the $^6H_{5/2}$→$^4F_{7/2}$ transition was observed in the PLE spectrum of the ZnMoO$_4$:Sm^{3+} phosphor.

Fig. 4 portrays the PL spectra of theZnMoO$_4$ phosphors by the functioning of different Sm^{3+} amounts in the 525-750 nm region. These PL spectra stimulated at 402 nm show four PL bands at 708, 649, 602 and 567 nm, that refer to the Sm^{3+} $^4G_{5/2}$→$^6H_{11/2}$ (red), $^6H_{9/2}$ (reddish orange), $^6H_{7/2}$ (orange) and $^6H_{5/2}$ (yellow) transitions in that order [2,4,27]. The transition from $^4G_{5/2}$ to $^6H_{7/2}$, which is linked to emission at 602 nm, has the highest intensity of all the other transitions and it might be widely exploited to create orange-orange luminous devices [2]. The intensity of PL increased when the concentration of Sm^{3+} in ZnMoO$_4$:Sm^{3+} increased from 0.5 to 1.5 mol%; however, the concentration decreased when doped with 2.0% of Sm^{3+} [4]. The levels $^4G_{5/2}$→$^6H_{11/2}$, $^6H_{9/2}$, $^6H_{7/2}$ and $^6H_{5/2}$ are restricted due to the prevention of ED transfer (ΔJ = ± 3), electric dipole, ED (ΔJ = ± 2), partially magnetic and partially electric dipole (ΔJ = ± 1) and magnetic dipole, MD (ΔJ = ± 0) transitions in nature, respectively [2,28-30]. The local site symmetry of Sm^{3+} ions in the ZnMoO$_4$ phosphor can be evaluated from the relative intensities of magnetic dipole (MD) and electric dipole (ED) transitions. The simultaneous observation of prominent MD and ED transitions implies that Sm^{3+} ions are distributed over both centrosymmetric and non-centrosymmetric lattice sites in the ZnMoO$_4$ host matrix.

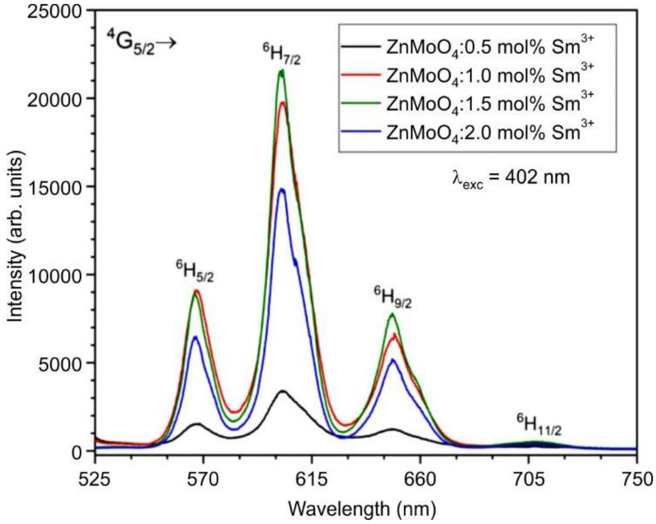

Fig. 4. PL spectra of Sm^{3+}-doped ZnMoO$_4$ phosphors

All possible emissions of present ZnMoO4:Sm^{3+} phosphors are described using an energy level diagram as shown in Fig. 5. The ions Sm^{3+} transition from the fundamental state $^6H_{5/2}$ to the level $^6P_{3/2}$ through an excitation at 402 nm. Significantly, the Sm^{3+} concentration below the threshold of 1.5 mol% in the ZnMoO$_4$ phosphor indicates a non-radiative (NR) energy transfer *via* relaxation channels (CR). Consequently, non-radiative (NR) decay occurs from the $^6P_{3/2}$ to $^4G_{5/2}$ state occurs, resulting in radiative emissions at 708, 649, 602 and 567 nm.

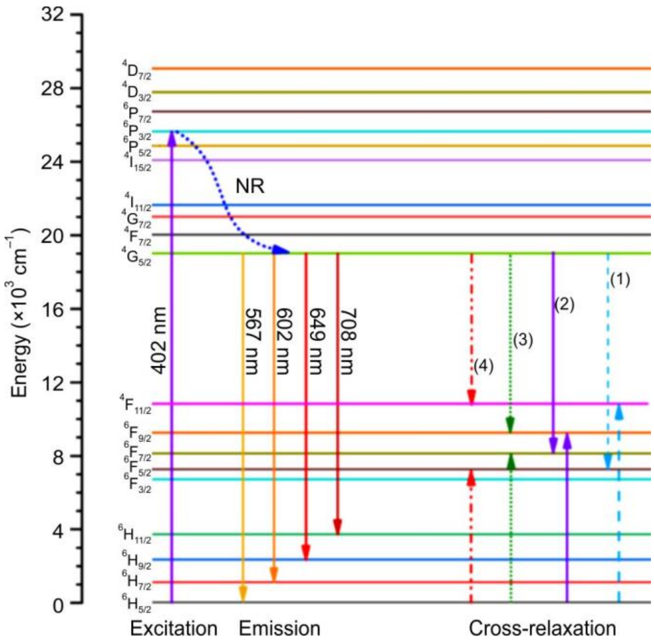

Fig. 5. Schematic energy level diagram of Sm^{3+} ions in ZnMoO$_4$:Sm^{3+} phosphors

Decay analysis: The fluorescence decays of $^4G_{5/2}$ emission (602 nm) for the different Sm^{3+} amounts doped $ZnMoO_4$ phosphors were measured under the stimulation at 402 nm as depicted in Fig. 6 for the non-exponential decay behaviour of the current $ZnMoO_4$:Sm^{3+} phosphors. The $^4G_{5/2}$ durations in $ZnMoO_4$ phosphorus with varying Sm^{3+} ion concentrations (0.5, 1.0, 1.5 and 2.0 mol%) are established as follows: 1.23, 1.19, 1.11 and 1.09 ms, respectively. The shorter lifespan of the $ZnMoO_4$:Sm^{3+} ferroborons may be due to stronger interactions between the Sm^{3+} ions [31,32].

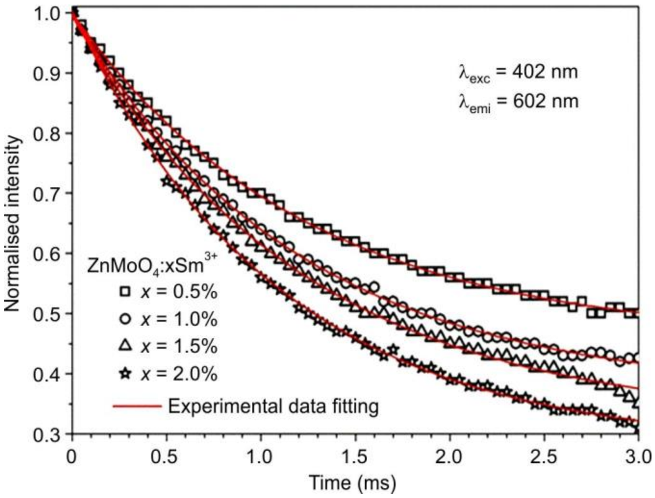

Fig. 6. Fluorescence decay of $ZnMoO_4$ phosphors with different amounts of Sm^{3+} ions

Colorific properties: Based on the results of photoluminescence, the colorimetric behaviour of $ZnMoO_4$ was also studied from the concentration of Sm^{3+} (Fig. 7). The colour coordinates (x, y), colour purity (CP) and correlated colour temperature (CCT) were analyzed. The (x, y) values obtained for the present synthesised phosphors are located in reddish-orange region as it is shown in Fig. 7. The (x, y) values are found to be (0.5545, 0.4414), (0.5840, 0.4148), (0.5920, 0.4071) and (0.6031, 0.3902) for the $ZnMoO_4$:0.5 mol% Sm^{3+}, $ZnMoO_4$: 1.0 mol% Sm^{3+}, $ZnMoO_4$: 1.5 mol% Sm^{3+} and $ZnMoO_4$:2.0 mol% Sm^{3+} phosphors.

The current values of $ZnMoO_4$:Sm^{3+} (x, y) are compared with the other Sm^{3+}-doped phosphors [2,3,7,33,34] in Table-1. As seen in Table-1, the present $ZnMoO_4$:1.5Sm^{3+} phosphor exhibits a maximum CP value of approximately 97%. Moreover, the CCT values of present $ZnMoO_4$:Sm^{3+} phosphors can be evaluated by using the McKamy's empirical formula [35,36]:

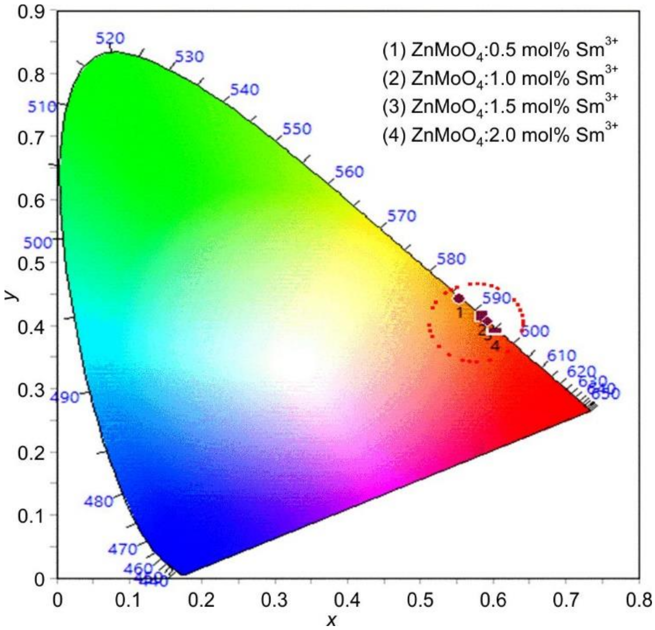

Fig. 7. CIE colour coordinates of ZnMoO4:Sm^{3+} phosphors as a function of Sm^{3+} amounts

$$CCT = -449n^3 + 352n^2 - 6823.2n - 5520.3 \qquad (2)$$

where n = (x – xe)/(y – ye); xe = 0.332, ye = 0.186.

The calculated CCT values for $ZnMoO_4$ doped with 0.5, 1.0, 1.5, and 2.0 mol% Sm^{3+} were found to be 1949, 1617, 1535, and 1276 K, respectively. These characteristics values obtained for the present $ZnMoO_4$:Sm^{3+} phosphors with CCT < 2000 K may suggest a potential application in warm-LEDs.

Conclusion

In summary, near-UV stimulated Zn(1-x)MoO_4:$x$$Sm^{3+}$ phosphors with various Sm^{3+} amounts (x = 0.5, 1.0, 1.5 and 2.0 mol%) were synthesised by a low temperature-initiated citrate gel combustion method. The triclinic structure with a crystallite size of 20 nm for the present $ZnMoO_4$:Sm^{3+} phosphors was confirmed by an XRD study. When stimulated to 402 nm, the PL spectra of the $ZnMoO_4$:Sm^{3+} phosphors exhibit four emission transitions: $^6H_{5/2}$ (yellow), $^6H_{7/2}$ (orange), $^6H_{9/2}$ (reddish orange) and $^6H_{11/2}$ (red), all of which correspond to Sm^{3+}. Dexter & Schulman's theory states that the photo-

TABLE-1
COMPARISON OF CIE (x, y), CP AND CCT VALUES OF Sm^{3+}–DOPED PHOSPHORS

Glass	(x, y)	CP (%)	CCT (K)	Ref.
$ZnMoO_4$:0.5 mol% Sm^{3+}	(0.554, 0.441)	92	1949	This work
$ZnMoO_4$:1.0 mol% Sm^{3+}	(0.584, 0.414)	95	1617	This work
$ZnMoO_4$:1.5 mol% Sm^{3+}	(0.592, 0.407)	96	1535	This work
$ZnMoO_4$:2.0 mol% Sm^{3+}	(0.603, 0.390)	97	1276	This work
$LiCaBO_3$:0.01 mol%Sm^{3+}	(0.560, 0.400)	96	–	[3]
$CaTiO_3$:2 mol%Sm^{3+}	(0.580, 0.420)	87	1975	[33]
KYBO:0.5 mol%Sm^{3+}	(0.511, 0.445)	93	1985	[7]
$Gd_{0.95}AlO_3$:0.05 mol% Sm^{3+}	(0.529, 0.484)	90	–	[34]
$NaY(MoO_4)$:0.1 mol% Sm^{3+}	(0.637, 0.355)	–	–	[37]
$CaMoO_4$:0.05 mol% Sm^{3+}	(0.590, 0.408)	–	300	[38]

luminescence (PL) reduction in current $ZnMoO_4:Sm^{3+}$ phosphors is caused by a dipole-dipole kind of interaction. The decomposition times for Sm^{3+} concentrations of 0.5, 1.0, 1.5 and 2.0 mol% in $ZnMoO_4$ are, respectively, 1.23, 1.19, 1.11 and 1.09 ms. The orange-red emission can be evaluated based on CIE (x, y) coordinates close to (0.60, 0.40) and a correlated colour temperature (CCT) below 2000 K, which are characteristic of warm-colour LED emission.

ACKNOWLEDGEMENTS

Two of the authors, BDPR and TCH, are grateful to the Rashtriya Uchchatar Shiksha Abhiyan (RUSA), Phase-II, Government of India, for the financial support provided through the Research Project No. UGC-III (7) RP/RUSA/2025, dated 29.07.2025.

CONFLICT OF INTEREST

The authors declare that there is no conflict of interests regarding the publication of this article.

DECLARATION OF AI-ASSISTED TECHNOLOGIES

During the preparation of this manuscript, the authors used an AI-assisted tool(s) to improve the language. The authors reviewed and edited the content and take full responsibility for the published work.

REFERENCES

1. Z. Xiao, J. Ye, B. Wu, F. Wang, J. Li, B. Zhang, W. Liu, L. Han and W. You, *Appl. Phys., A Mater. Sci. Process.*, **128**, 120 (2022); https://doi.org/10.1007/s00339-021-05218-w
2. V. Singh, A. Yadav, C.B. Annapurna Devi, A.S. Rao and N. Singh, *Optik*, **242**, 167264 (2021); https://doi.org/10.1016/j.ijleo.2021.167264
3. M. Sharma, H. Sharma, I. Charak, H.C. Swart and V. Kumar, *Chem. Phys. Impact.*, **9**, 100696 (2024); https://doi.org/10.1016/j.chphi.2024.100696
4. H. Guo, B. Devakumar, R. Vijayakumar, P. Du and X. Huang, *RSC Adv.*, **8**, 33403 (2018); https://doi.org/10.1039/C8RA07329E
5. R. Cao, W. Wang, Y. Ren, Z. Hu, X. Zhou, Y. Xu, Z. Luo and A. Liang, *J. Lumin.*, **235**, 118054 (2021); https://doi.org/10.1016/j.jlumin.2021.118054
6. B. Goswami, R. Ahlawat and S. Devi, *J. Mater. Sci.*, **58**, 18029 (2023); https://doi.org/10.1007/s10853-023-09151-6
7. G. Sowjanya, R. Doddoji and V.R. Minnam Reddy, *Radiat. Phys. Chem.*, **190**, 109791 (2022); https://doi.org/10.1016/j.radphyschem.2021.109791
8. V. Chauhan, P.K. Pandey, P. Dixit, P. Deshmukh, S. Satapathy and P.C. Pandey, *J. Lumin.*, **248**, 118994 (2022); https://doi.org/10.1016/j.jlumin.2022.118994
9. A.B. Chavan, A.B. Gawande, V.B. Gaikwad, G.H. Jain and M.K. Deore, *J. Lumin.*, **234**, 117996 (2021); https://doi.org/10.1016/j.jlumin.2021.117996
10. M.G. Nikolić, D.J. Jovanović, V. Đorđević, Ž. Antić, R.M. Krsmanović and M.D. Dramićanin, *Phys. Scr.*, **T149**, 014063 (2012); https://doi.org/10.1088/0031-8949/2012/T149/014063
11. H. Seshagiri Rao, P. Nagaraja, S. Sharma, G.R. Rao and P. Justin, *Mater. Today Sustain.*, **27**, 100932 (2024); https://doi.org/10.1016/j.mtsust.2024.100932
12. B. Singh, A. Tamta, B. Chandra, N.D. Kandpal, S.S. Jadaun, A.K. Panwar, K.V. Babu, P. Justin, H. Seshagiri Rao and K.S.K.R.C. Sekhar, *Ceram. Int.*, **49**, 38047 (2023); https://doi.org/10.1016/j.ceramint.2023.09.135
13. H. Gurusamy, R. Sivasubramanian, Y. Johnbosco and M. Bhagavathiachari, *Chem. Pap.*, **75**, 1715 (2021); https://doi.org/10.1007/s11696-020-01420-x
14. R. Roshani and A. Tadjarodi, *Mater. Today Commun.*, **26**, 101794 (2021); https://doi.org/10.1016/j.mtcomm.2020.101794
15. F.B. Xiong, H. Chen, H.F. Lin, X.G. Meng, E. Ma and W.Z. Zhu, *J. Lumin.*, **209**, 89 (2019); https://doi.org/10.1016/j.jlumin.2019.01.034
16. P.K. Pandey and P.C. Pandey, *J. Lumin.*, **242**, 118600 (2022); https://doi.org/10.1016/j.jlumin.2021.118600
17. S. Wang, H. Zhang, T. Wang, H. Lv, X. Zou, Y. Wei, W. Hu and C. Su, *J. Alloys Compd.*, **823**, 153822 (2020); https://doi.org/10.1016/j.jallcom.2020.153822
18. A. Herrera, A. Becerra and N. M. Balzaretti, *J. Lumin.*, **188**, 193 (2017); https://doi.org/10.1016/j.jlumin.2017.04.033
19. V. Chauhan, P. Dixit and P.C. Pandey, *J. Rare Earths*, **39**, 1336 (2021); https://doi.org/10.1016/j.jre.2020.10.014
20. P.K. Vishwakarma, A. Bahadur, A. Maurya and S.B. Rai, *Mater. Res. Bull.*, **115**, 219 (2019); https://doi.org/10.1016/j.materresbull.2019.03.029
21. Y.N. Rajeev, K. Venkatarao, B.V.N. Kumar, L.B. Kumar and S. Cole, *Mater. Today Proc.*, **49**, A1 (2022); https://doi.org/10.1016/j.matpr.2021.12.554
22. Y. Liang, P. Liu, H.B. Li and G.W. Yang, *Cryst. Growth Des.*, **12**, 4487 (2012); https://doi.org/10.1021/cg3006629
23. N. Maheswari and G. Muralidharan, *Appl. Surf. Sci.*, **416**, 461 (2017); https://doi.org/10.1016/j.apsusc.2017.04.094
24. D. Chen, M. Liu, L. Yin, T. Li, Z. Yang, X. Li, B. Fan, H. Wang, R. Zhang, Z. Li, H. Xu, H. Lu, D. Yang, J. Sun and L. Gao, *J. Mater. Chem.*, **21**, 9332 (2011); https://doi.org/10.1039/c1jm11447f
25. R.L. Frost and S.J. Palmer, *J. Raman Spectrosc.*, **42**, 2042 (2011); https://doi.org/10.1002/jrs.2959
26. Z. Wang, H. Liang, M. Gong and Q. Su, *Opt. Mater.*, **29**, 896 (2007); https://doi.org/10.1016/j.optmat.2005.12.010
27. H. Li, X. Gong, Y. Chen, J. Huang, Y. Lin, Z. Luo and Y. Huang, *J. Rare Earths*, **36**, 456 (2018); https://doi.org/10.1016/j.jre.2017.09.014
28. A.N. Kumar, D.M. Jnaneshwara, H. Nagabhushana, C. Pratapkumar, C.R. Ravikumar, M.R.A. Kumar, T.R.S. Shekhar and S.C. Prashantha, *Appl. Surf. Sci. Adv.*, **4**, 100070 (2021); https://doi.org/10.1016/j.apsadv.2021.100070
29. R. Mahajan and R. Prakash, *Mater. Chem. Phys.*, **246**, 122826 (2020); https://doi.org/10.1016/j.matchemphys.2020.122826
30. A. Balakrishna, H.C. Swart, R. Ramaraghavulu, A.K. Bedyal, R.E. Kroon and O.M. Ntwaeaborwa, *J. Alloys Compd.*, **727**, 224 (2017); https://doi.org/10.1016/j.jallcom.2017.08.117
31. B. Han, B. Liu, Y. Dai and J. Zhang, *Mater. Res. Bull.*, **121**, 110612 (2020); https://doi.org/10.1016/j.materresbull.2019.110612
32. M. Xie, X. Min, Z. Huang, Y. Liu, X. Wu and M. Fang, *Chem. Phys. Lett.*, **710**, 84 (2018); https://doi.org/10.1016/j.cplett.2018.08.080
33. P. Singh, S. Modanwal, H. Mishra and S.B. Rai, *RSC Adv.*, **13**, 22663 (2023); https://doi.org/10.1039/D3RA04468H
34. P. Kumar, D. Singh, I. Gupta, S. Singh and V. Kumar, *Chem. Phys. Lett.*, **812**, 140277 (2023); https://doi.org/10.1016/j.cplett.2022.140277
35. I. Jlassi, R. Doddoji, S. Brahem, B. Gelloz, V.R. Minnam Reddy and S. Alhammadi, *J. Lumin.*, **275**, 120810 (2024); https://doi.org/10.1016/j.jlumin.2024.120810
36. P. Meejitpaisan, R. Doddoji, S. Kothan, H.J. Kim, V.R. Minnam Reddy, S. Alhammadi and J. Kaewkhao, *Mater. Res. Bull.*, **185**, 113295 (2025); https://doi.org/10.1016/j.materresbull.2025.113295
37. B. Qi, B. Mu, J. Huang, R. Song and Y. Dong, Optical Analysis of Dy^{3+}/Sm^{3+} Co-Doped $Nay(MoO_4)_2$ Phosphors for Warm White Led *SSRN* (2022); https://doi.org/10.2139/ssrn.4260090
38. W.-T. Wu, K.-K. Tiong, Y.-W. Lee, S.-Y. Hu, Y.-C. Lee and W. Huang, *Appl. Sci.*, **12**, 7883 (2022); https://doi.org/10.3390/app12157883